Open Archive Toulouse Archive Ouverte (OATAO)

OATAO is an open access repository that collects the work of Toulouse researchers and makes it freely available over the web where possible.

This is an author-deposited version published in: http://oatao.univ-toulouse.fr/
Eprints ID: 8882

Any correspondence concerning this service should be sent to the repository administrator: staff-oatao@listes-diff.inp-toulouse.fr

Identification of elastomers by Digital Image Correlation

M. Fazzini, S. Mistou & M. Karama
Laboratoire Genie de Production, Ecole Nationale d'Ingenieurs de Tarbes, BP1629, 65016 Tarbes, France

B. Desmars & P. Peres
EADS SPACE, BP11, 33165 Saint-Medard-en-Jalles, France

ABSTRACT: As a complement to classic characterization in the identification of elastomers, full-field measurement methods such as digital image stereo correlation can undeniably contribute to the validation of elastomeric connection behavior. Indeed, these measurements enable three-dimensional displacement and strains fields over the totality of the studied surface to be finely reached. Characterization tests in shearing on an elastomer were followed by image stereo correlation up to high strain levels. The experimental results could thus be compared with theoretical results using an Alexander hyper-elastic constitutive law, which enabled the relevance of this law to be validated locally.

1 INTRODUCTION

In the sector of civil and military launchers, some structural connections are in elastomer. There may be several reasons leading to the choice of such connections : balance of strain difference between the two substrates, filtering of high frequency dynamic phenomena, impossibility of transferring loading via riveted or bolted connections (tanks for example). The sizing and justification of such connections require perfect knowledge of modeling their behavior for diverse cases of multi-axial mechanical loading to which they are generally subjected.

This in turn makes is necessary to possess the relevant constitutive models of elastomer to be able to represent its quasi-incompressible hyper-elastic behavior for the various types of loading. In addition, the constitutive laws of these bonded connections are generally produced by optimization in order to adjust the elastomer behavior under certain simple types of loading (uni-axial tensile and compression, simple shear, equi-biaxial tensile …).

Classical measurement generally used for such characterization gives access only to global and macroscopic values useful for the description of the behavior model. However, this method does not enable the relevance of the constitutive law to be judged in particular areas such as the connection end. These areas, however, often seem distinct at the time of validation because of edge effects and loads transmitted by the elastomer in meniscus areas. As a complement to the characterization carried out generally to describe the behavior of the elastomer, an optical measurement method without contact such as image stereo correlation can contribute considerably to mastering the modeling and sizing of elastomeric connections (Chevalier & Marco 2002, Laraba-Abbes et al. 2003).

Indeed, these measurements provide accurate access to displacement and strain fields over the totality of the measured area and especially to areas in which meniscus effect appears. Thus, quadruple shearing tests on an elastomer (acryloNitrile Butadiene Rubber) were followed by image stereo correlation up to high warping levels (200%). Experimental results obtained by this technique could thus be compared with theoretical analysis using the hyper-elastic behavior laws selected for this material. The aim of this comparison is to evaluate the relevance of this law as far as current areas and meniscus areas are concerned.

2 GLOBAL CHARACTERIZATION OF THE BEHAVIOR OF ELASTOMER

2.1 *Hyper-elastic potentials*

The hyper-elastic behavior laws (strain-stress relations) are formulated from hyper-elastic potentials (density of strain energy). These densities of strain energy, often called W, are written starting from the invariables of the Cauchy Green elongation tensor (I_1, I_2 and I_3) or directly from the main elongations (λ_1, λ_2 and λ_3). In these relations, coefficients C_i which represent the mechanical properties of the material computed also intervene:

$$W(C_i, I_1, I_2, I_3) \text{ or } W(C_i, \lambda_1, \lambda_2, \lambda_3) \qquad (1)$$

The components of the Piola Kirchhoff second stress tensor S is then obtained by derivation of the density of strain energy:

$$S = 2\frac{\partial W}{\partial C} = 2\left[\frac{\partial W}{\partial I_1}\frac{\partial I_1}{\partial C} + \frac{\partial W}{\partial I_2}\frac{\partial I_2}{\partial C} + \frac{\partial W}{\partial I_3}\frac{\partial I_3}{\partial C}\right] \quad (2)$$

The constitutive law used in the following paper is the Alexander law (eq.3). This law was preferable to more traditional laws used to model elastomer behavior (Mooney-Rivlin, Haynes-Wilson …) because of its capacity to represent well the non-linear shear behavior. This law is represented by the following hyper-elastic potentials (Alexander 1968):

$$W(I_1, I_2, I_3) = C_1\int_0^{I_1} \exp K.(I_1-3)^2 dI_1$$
$$+ C_2 \ln\left(\frac{I_2-3+\tau}{\tau}\right) + C_3(I_2-3) + k\left(\ln(I_3)\right)^2 \quad (3)$$

2.2 Alexander's law

Elementary characterization tests were implemented for various simple load cases on an NBR type elastomer: uni-axial tensile and compression, simple shear, pure shear and equi-biaxial tensile. The parameters of the Alexander law were determined by optimization in order to adjust as well as possible all experimental curves for these various load cases (Mistou et al. 2004).
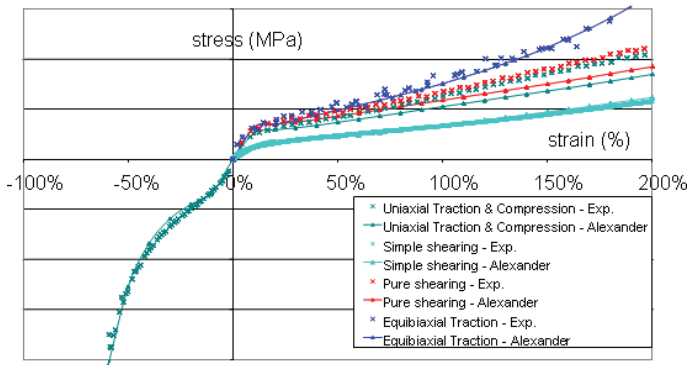

Figure 1. Comparison between Alexander's law and experimental elementary tests.

This constitutive law enables the macroscopic behavior of the elastomer to be represented in simple shearing (Figure 1) with in particular a good representation of the stiffening at weak warping, uni-axial compression and equi-biaxial tensile. The compressibility coefficient of the elastomer is characterized by hydrostatic compression tests (Piron & Soufflet 2006). On the other hand, the relevance of this law is not validated in various distinct areas: connection ends, meniscus areas…

3 FOLLOW-UP OF QUADRUPLE SHEARING TESTS BY STEREO-CORRELATION

3.1 Stereo-correlation

Image correlation allows the measurement of displacement fields of a planar surface: a single camera acquires a sequence of images of a planar object under plane strain. Displacements of points distributed over the surface of the object are calculated from the grey level analysis of the images (Wattrisse et al. 2001). Given two images corresponding to two deformation states of an object, to determine the correspondent of a point and its signature of the first image in the second, a similarity function is used. In practice, a single value is not the unique signature of a point, hence neighboring pixels are used. The matching of images acquired by only one camera, at different times, on an object which becomes deformed is called temporal matching, or tracking. From its principle, the correlation technique can function correctly only with objects having a surface with a sufficiently random texture. If the object is not naturally textured or if its texture is not sufficiently discriminating, various techniques exist to allow the use of correlation (paint projection).

Image correlation presents two major disadvantages: firstly, it enables only plane deformations to be measured; then, from an experimental point of view, it requires the deformation plane and the image plane of the camera to be parallel and remain so during the test, but this is difficult to guarantee. The technique of stereovision brings a solution to these two problems. The use of two cameras enables three-dimensional information to be reached (Orteu 2002).

Stereovision is based on the principle that the depth information (3D) can be obtained by triangulation starting from two images having a common part in their field of sight (McNeill et al. 1997, Garcia et al. 2002). Obtaining this data involves the calibration of the stereoscopic vision sensor. The calibration of a camera is an important stage in dimensional metrology by artificial vision. Calibrating a camera consists in determining its intrinsic parameters. Calibrating a stereovision sensor made up of two dependent cameras involves determining the intrinsic parameters of each camera, as well as the position and relative orientation of both cameras. These calibration parameters are necessary to calculate, by triangulation, the three-dimensional co-ordinates of a point corresponding to pixels matched in the two images. The matching of two acquired images, at a given moment, by two dependent stereoscopic cameras is called matching by stereo-correlation. The measurement of 3D displacement fields using stereovision implements simultaneously a temporal matching technique and a stereo-correlation matching. The correlation technique can also be used to

seek stereo-correspondents starting from a pair of stereoscopic images. Note that an essential difference distinguishes temporal matching by correlation from matching by stereo-correlation: in the case of the stereovision, there is a geometrical constraint known as epipolar which can guide research into the stereo-correspondent.

3.2 Experimental device

Two digital cameras acquire digital images with a 1280 by 1024 pixel definition. These images are then computed by Aramis 3D software (GOM mbH). This device makes it possible to measure displacement and strain on the surface of an object with a resolution of 500 to 1000 μm/m in strain. Calibration is the fundamental stage which precedes frame grabbing. A calibration plate of a size equivalent to the measurement surface is placed at a fixed distance. During this process, several images of the plate are taken in various positions. The calibration plate is constellated with white points at known distances. The precision obtained during calibration is lower than the pixel, which corresponds to an error of a few microns in displacement. Aramis software is able to recognize the points of an image by grey level analysis, through the application on the measured object of black and white paint which generates the variable grey levels on the surface of the object. A grey level figure coded on 8 bits corresponds to each pixel of the CCD sensor. A succession of several pixels taken on the same line forms a grey level sequence called grey level distribution. The fundamental principle lies in the fact that the distribution does not vary during deformation of the object. It is therefore sufficient to follow this distribution of grey levels in their movement to obtain displacements of the object. In practice, this is made possible by correlation domains which are 15x15 pixel gathering zones.

The definition of samples is taken from the standard NFT46.020 on the determination of the adherence of elastomer using the sample called quadruple shear (Figure 2). The warping is defined by the ratio between half displacement and the thickness of the elastomer. The results analysis area is 11x13 millimeters. By taking into account half displacement of quadruple shear testing (approximately 10 millimeters), we used a calibration plate of 20x25 millimeters as shown in Figure 2. The calibration of the measurement device was carried out with 50 millimeters objectives. The calibration distance (standard distance on the calibration plate) is 15 millimeters. The measurement distance (distance between sample and cameras) is approximately 255 millimeters. The calibration error for the various samples varies from 0.02 to 0.04 pixels: i.e. approximately one micrometer in displacement. The automatic frame grabbing of the measurement device (controlled by the analogical output of the tensile testing machine) was set for a warping increment of 10%.
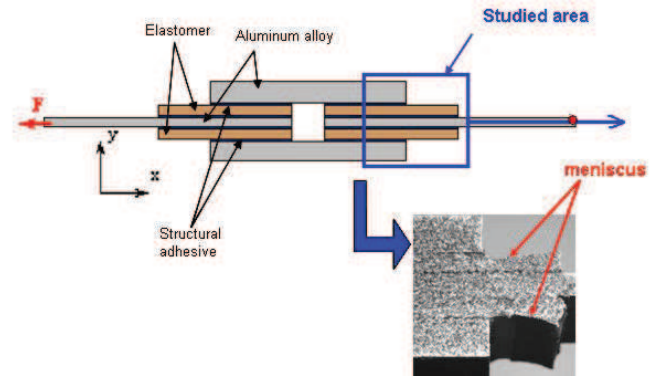

Figure 2. Quadruple shearing sample and studied area.

The quality of images and grey levels applied on the structures are the basis of the computation carried out by the Aramis software. The grey levels are usually created by the application of black and white paint on the measurement area. On the other hand, it is necessary to apply as little paint as possible in order to measure the deformations of the object and not those of the painting (Mistou et al. 2003).

A grey level on the first sample was applied using standard black and white paint (Figure 2). During the test, the grey levels disappear because of the high warping of the elastomer, which induces paint peeling. For the others tests, the grey level was applied using black paint and white silicone. The coat of black paint is thin on the elastomer, silicone is used for its characteristics of elongation under deformation. This configuration enabled (during calculation) results with considerable warping (250%) to be reached. The third test enabled the testing of a configuration without the application of black paint on the elastomer (which is naturally dark grey). The grey level is applied using white silicone only, and the natural color of the elastomer. During the test, the elastomer whitened under deformation, which made it impossible to treat results with high warping.

Strain calculation is carried out from the displacement measurement using the Green-Lagrange strain tensor. Contrary to small perturbation assumptions, this tensor enables additional terms for large deformations to be taken into account. In order to calculate displacements and strains, for all acquisitions there is a calculation point every 11 pixels, the size of which is 15x15 pixels (correlation window). The strain calculation is carried out with the multi-facet method using nine correlation windows, i.e. the displacement derivative is carried out over an area of 22x22 pixels.

4 EXPERIMENTAL ANALYSIS

4.1 *Experimental results*

Elastomer failure was observed for an average load of 18000 Newton and a machine displacement of approximately 25 millimeters (450% warping). The behavior of the sample is non-linear elastic (Figure 3). Failure was observed successively for right inferior and left superior elastomer.
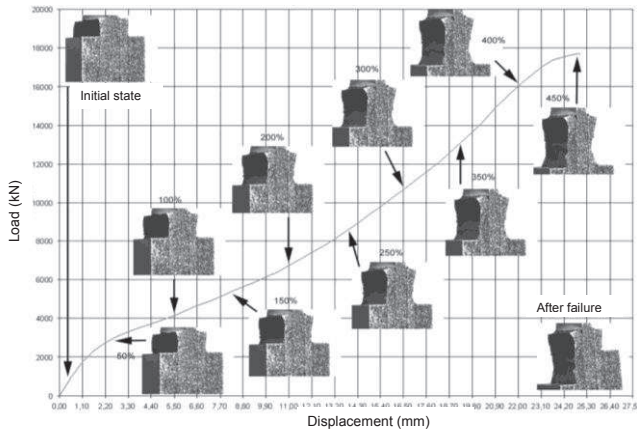

Figure 3. Load-displacement curve.

This study relates to the experimental results obtained for warping (shear strain $\gamma_{xy}/2$ in degrees) compared to theoretical warping (in %). In general, the information is entirely available at any point of the elastomer up to theoretical warping of 200% and is partially exploitable up to 250%. All the results presented are provided by the computation carried out by the Aramis software, without the use of filtering in post-processing.

Figure 4 presents the experimental results obtained for theoretical warping of 100% in displacements for the three directions (Displ.X : displacement perpendicular to the tensile direction, Displ.Y : displacement in the tensile direction, Displ.Z : displacement perpendicular to the measurement surface); and in strains on the measurement surface (Epsilon X : strain along X-axis, Epsilon Y : strain along tensile Y-axis, Shear Angle : shear strain in the XY-plane).

The stereo-correlation measurement enables the results to be displayed over the whole measurement surface, including the edges of the sample. It also makes it possible to get the displacement perpendicular to the measurement surface, which is not possible in a two-dimensional study. For displacement of approximately 2.75 mm a thinning down of the elastomer of approximately 1.25 mm is to be noted. Normal strains, as well as shear strain approach or exceed 100%, i.e. 1 m/m.
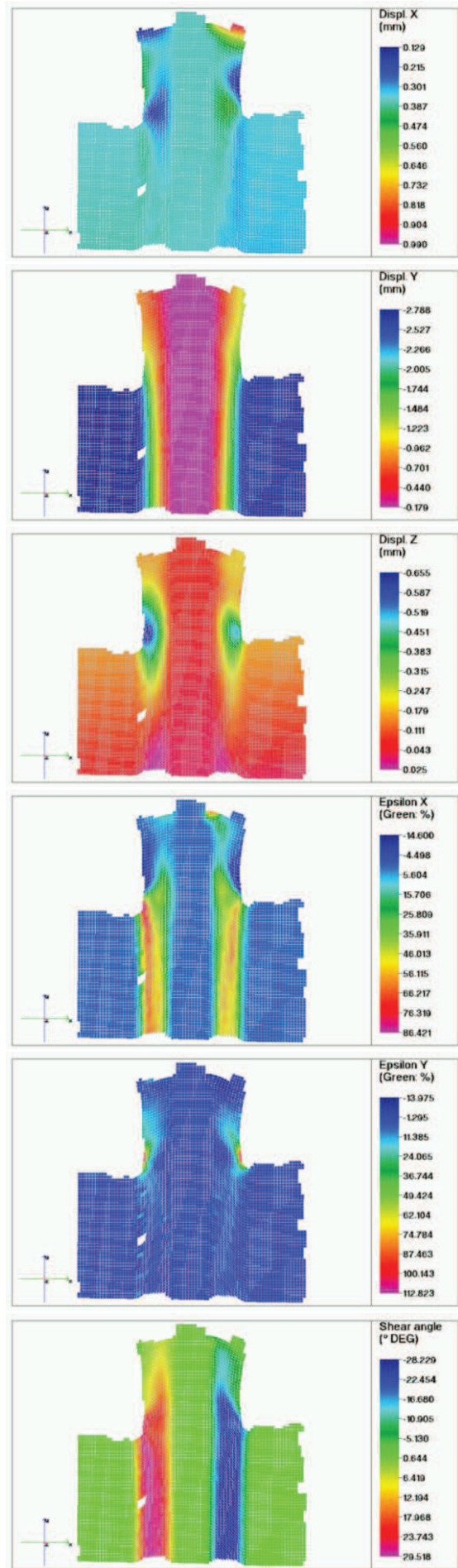

Figure 4. Experimental displacements and strain results for a theoretical warping of 100%.

4.2 Reproductibility of the experimental results

In order to appreciate the reproduction possibility of the tests, the displacements fields obtained on three samples were superimposed on the same warping level (100%) on the line shown on the Figure 5.
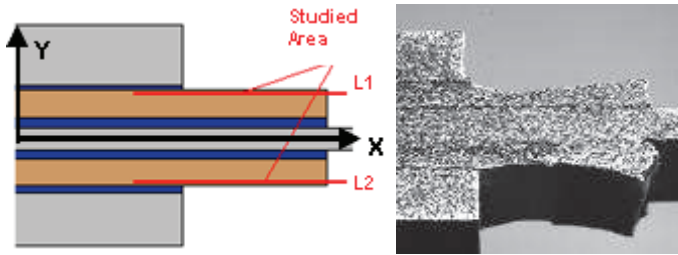

Figure 5. Measurement exploitation (studied area and local bonding defects).

The comparison of the results obtained on the six connections tested (two connections studied per sample) illustrates the considerable incidence of local defects (lack of bonding at end of over length – Figure 5) on the strains within the elastomer as presented in Figure 6. In the continuation of the study, only the results of the third sample were taken into account, this sample presenting the lowest number of local defects among those studied (the defects noted during the test were finally taken into account in the modeling).
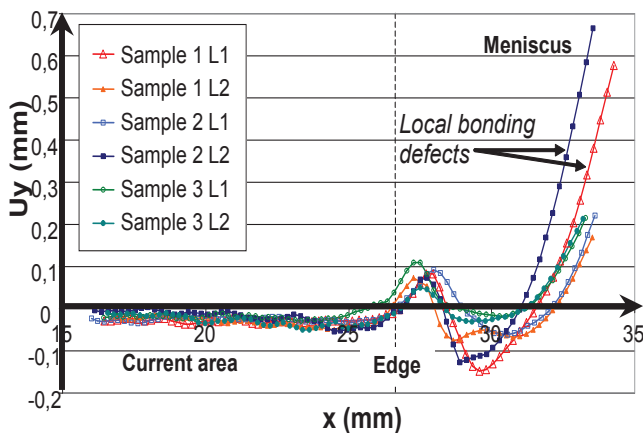

Figure 6. Superposition of the experimental results.

5 CONFRONTATION WITH THE THEORETICAL RESULTS (FEA)

5.1 Plane stress and 3D FEA

A finite element analysis of the behavior of the quadruple shearing sample was carried out by introducing the previously described Alexander's law. This analysis was carried out in non-linear under the SAMCEF Mecano module software under the plane-stress assumptions (Alex CP) and 3D (Alex 3D). The aim of these comparisons is to check the relevance of the behavior law retained both at global and at local level. Comparisons between numerical and experimental results as a whole were carried out ar-

bitrarily at a warping level of 100%. The curves given below show the evolution of the theoretical displacements along the axes of the reference coordinate system defined in Figure 5 for lines at various thicknesses of the elastomer (i.e. at Y constant from the X-axis, half-thickness of aluminium is 1.5 mm).
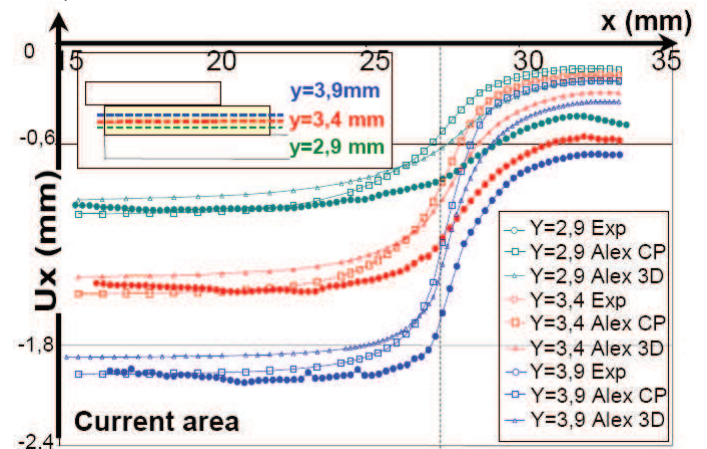

Figure 7. Comparison of FEA results in plane stress and in 3D.

These comparisons (Figure 7) make it possible to note that the plane stress assumption is not entirely suitable. In the continuation of the study, the results obtained with the 3D model were therefore presented, by introducing the defects noted after realising the samples (in particular a joining defect in end of over length).

5.2 Strain analysis

The exploitation of displacements in the elastomer thickness initially enables readjustment of the modelling assumptions (Young modulus, working thickness) and also an initial idea of the thickness of the interphase zone (elastomer zone with adhesive) to be obtained. The Figure 8 presents the superimposition of the strain fields (according to Green-Lagrange) obtained experimentally and numerically (from the model adapted in thickness including failure of 0.9 mm). The behaviour law used for the elastomer is well suited for reporting displacement and strain.
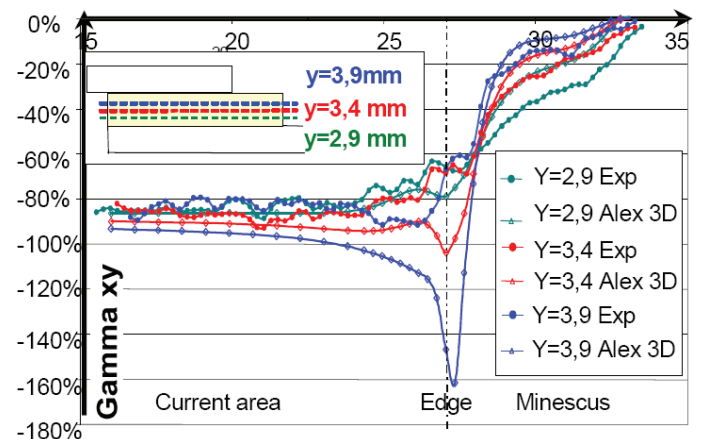

Figure 8. Theoretical (FEA) and experimental shear strain field.

5.3 Numerical edge effect

This comparison highlights over-stress phenomenon at the end of plate during the analysis of theoretical results; this over-stress being characterized by strain peaks on all the terms of the Green-Lagrange strain tensor (Figure 8). However this phenomenon is not at all noted experimentally. The Figure 9 illustrates the fundamental deviation existing locally between the experimental and numerical data.
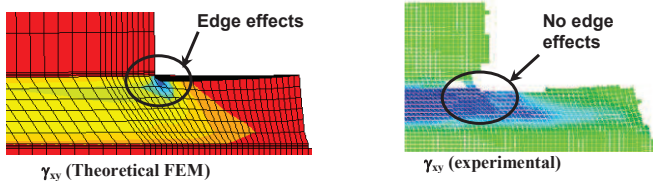

Figure 9. Theoretical (FEA) and experimental warping at end of connection.

A sensitivity study of the meshing in FE showed that this phenomenon was exacerbated when the mesh was refined. Various attempts (modeling of the adhesive with an elasto-plastic law, modeling of a connection between external plate and over length) did not enable to erase this local behavior variation. In conclusion, since theoretical over-stress is to be found on some elements in elastomer and because the experimental results do not show this phenomenon at all, this phenomenon is likely to have a primarily numerical origin.

In order to justify this result we used another full-field measurement technique called Electronic Speckle Pattern Interferometry (ESPI), which is used more particularly in the case of field measurements of small displacements and strains. Given that the numerical stress peak occurs whatever the load; the measurement by ESPI was carried out for theoretical warping lower than 5%. By this experimental measurement the results obtained by image stereocorrelation can be confirmed; the stress peak is not identified, its origin is purely numerical.

6 CONCLUSION

Characterization tests in quadruple shearing on NBR-type elastomer were followed by image stereo-correlation up to high warping levels (over 200% warping). Reproducibility, reliability and accuracy of measurements were evaluated through several successive tests which showed that this technique was well-adapted to the full-field measurement of displacement and strain zones, up to 200% warping.

The experimental results obtained by this technique were then compared with the results of finite element analysis carried out in 3D for various warping levels. These analyses showed up good correlation between the experimental and theoretical (FEA) results.

In addition, the study of the FE mesh highlighted an edge effect phenomenon at the right end of the stuck support. Given the initial results, the numerical share of the edge effects seems considerable. Indeed measurements by stereo-correlation do not show any over-stress in this area. After a thorough study by ESPI, the conclusion of the numerical origin of the noted edge effects is confirmed.

This study illustrates the contribution which a non-contact full-field optical measurement method such as digital image stereo-correlation can make to the characterization for elastomer materials in large deformation.

7 REFERENCES

Alexander, H.A. 1968. Constitutive relation for rubber-like materials. *Int. Journal Engineering Science* 6: 549-563.

Chevalier, L. & Marco, Y. 2002. Tools for multiaxial validation of behavior laws chosen for modeling hyper-elasticity of rubber-like materials. *Polymer Engineering and Science* 42(2): 280-298.

Garcia, D., Orteu, J.J. & Penazzi, L. 2002. A combined temporal tracking and stereo-correlation technique for accurate measurement of 3D displacements: application to sheet metal forming. *Journal of Materials Processing Technology* 125-126: 736-742.

Laraba-Abbes, F., Ienny, P. & Piques, R. 2003. A new Tailor-Made methodology for the mechanical behavior analysis of rubber-like materials – Part I & II. *Polymer* 44: 807-840.

McNeill, S.R., Sutton, M.A., Miao, Z. & Ma, J. 1997. Measurement of surface profile using digital image correlation. *Experimental Mechanics* 37(1): 13-20.

Mistou, S., Karama, M., Dalverny, O., Siguier, J.M. & Guigue-Joguet, P. 2003. Mesure 3D sans contact des déplacements et déformations sur des films plastiques transparents par stéréo-corrélation. *Mécanique et Industrie* 4(6): 637-643.

Mistou, S., Karama, M., Desmars, B., Peres, P., Piron, E. & Heuillet, P. 2004. Application de la méthode de stéréocorrélation d'images à la caractérisation des élastomères en grandes déformations. *Revue Instrumentation Mesures Métrologie* 4(3-4): 147-166.

Orteu, J.J. 2002. Mesure 3D de formes et de déformations par stéréovision. *Techniques de l'Ingénieur, traité Génie Mécanique, BM7015.*

Piron, E. & Soufflet, L. 2006. Modélisation du comportement mécanique d'élastomères fortement non linéaires par des lois d'Alexander. *International Rubber Conference, 16-18 May 2006, Lyon.*

Wattrisse, B., Chrysochoos, A., Muracciole, J.M., & Nemoz-Gaillard, M. 2001. Analysis of strain localization during tensile tests by digital image correlation. *Experimental Mechanics* 41(1): 29-39.